European Journal of Mechanics B/Fluids 28 (2009) 744–752

Contents lists available at ScienceDirect

European Journal of Mechanics B/Fluids

journal homepage: www.elsevier.com/locate/ejmflu

MHD natural convection flow and heat transfer in a laterally heated partitioned enclosure

Kamil Kahveci*, Semiha Öztuna

Mechanical Engineering Department, Trakya University, 22180 Edirne, Turkey

ARTICLE INFO

Article history:
Received 20 August 2006
Received in revised form
16 June 2009
Accepted 15 July 2009
Available online 23 July 2009

Keywords:
Natural convection
MHD
PDQ
Enclosure
Partition

ABSTRACT

This study looks at MHD natural convection flow and heat transfer in a laterally heated enclosure with an off-centred partition. Governing equations in the form of vorticity–stream function formulation are solved using the polynomial differential quadrature (PDQ) method. Numerical results are obtained for various values of the partition location, Rayleigh, Prandtl and Hartmann numbers. The results indicate that magnetic field significantly suppresses flow, and thus heat transfer, especially for high Rayleigh number values. The results also show that the *x*-directional magnetic field is more effective in damping convection than the *y*-directional magnetic field, and the average heat transfer rate decreases with an increase in the distance of the partition from the hot wall. The average heat transfer rate decreases up to 80% if the partition is placed at the midpoint and an *x*-directional magnetic field is applied. The results also show that flow and heat transfer have little dependence on the Prandtl number.

1. Introduction

In many practical cases, enclosures with vertical partitions are used to modify heat transfer, and various numerical and experimental studies have been performed on this subject. In these studies, the effects of various geometrical and transport parameters such as aspect ratio, location of partition, inclination angle, and Rayleigh and Prandtl numbers on flow and heat transfer were examined. Anderson and Bejan [1] studied enclosures with single and double partitions theoretically and experimentally and obtained a correlation for heat transfer between the two ends of the enclosure. Ho and Yih [2] performed a numerical study of natural convection in an air-filled partitioned enclosure and concluded that the heat transfer rate is considerably attenuated in a partitioned enclosure relative to a non-partitioned enclosure. Tong and Gerner [3] observed that placing a partition midway between the vertical walls of an enclosure produces the greatest reduction in heat transfer. In another study, Dzodzo and Pavlovic [4] found that with a centred vertical partition, convective heat transfer could be reduced up to 64%. Elsherbiny et al. [5] found that the thermal boundary conditions at the end walls influence the effects of partitions in reducing the heat transfer rate across the enclosure. In their study, Acharya and Tsang [6] observed that the inclination angle has a strong influence on the magnitude of the maximum Nusselt number. Kahveci [7,8] found that the average Nusselt number decreases with increasing distance between the hot wall and the partition. Furthermore, he observed that with a decrease in the thermal resistance of the partition, the average Nusselt number shows an increasing trend, a peak point is detected, and then the average Nusselt number begins to decrease asymptotically to a constant value. Kahveci [7,8] also observed that the average heat transfer rate exhibits little dependence on the width of the partition. In another study, Kahveci [9] found that with increasing aspect ratio, heat transfer shows an increasing trend and reaches a maximum value. Beyond this maximum point, the trend reverses to decrease with further increases in aspect ratio.

As can be seen, previous studies have generally examined natural convection in the absence of a magnetic field. However, natural convection under the influence of a magnetic field is of great importance in many industrial applications such as crystal growth, metal casting and liquid metal cooling blankets for fusion reactors. In one of the limited numbers of studies on this subject, Kahveci and Öztuna [10] investigated the magnetohydrodynamic flow and heat transfer in a tilted enclosure with a centred partition and found that for high Rayleigh numbers, the average Nusselt number shows an increasing trend as the inclination angle increases and a peak value is detected. Beyond the peak point, the trend reverses to decrease with further increases in the inclination angle. The results of this study also show that the

* Corresponding author. Tel.: +90 284 2261217; fax: +90 284 2261225.
E-mail addresses: kamilk@trakya.edu.tr (K. Kahveci), semihae@trakya.edu.tr (Semiha Öztuna).

0997-7546/$ – see front matter © 2009 Elsevier Masson SAS. All rights reserved.
doi:10.1016/j.euromechflu.2009.07.001

Nomenclature

a	first-order weighting coefficient
B	magnetic induction
b	second-order weighting coefficient
g	gravitational acceleration
H	enclosure height
Ha	Hartmann number
i, j	grid point indices
L	enclosure width
ℓ	length
N_x	grid number along x direction
N_y	grid number along y direction
Nu	Nusselt number
Pr	Prandtl number
p	pressure
Ra	Rayleigh number
T	temperature
U	velocity
u, v	velocity components in x, y directions
w	width of the partition
x, y	coordinates
α	thermal diffusivity
β	thermal coefficient of volume expansion
δ	ratio of magnetic field strengths of x and y directions
Φ	dependent variable
ϕ	inclination angle
υ	kinematic viscosity
η	outward variable normal to the surface
ρ	density
σ	electrical conductivity of the fluid
ω	vorticity
ψ	stream function

Subscripts

a	average
C	cold
H	hot
p	partition
x	x-direction
y	y-direction

Superscripts

*	dimensional quantities
m	current iteration
+	right face of partition
−	left face of partition

Overlines

–	in y direction

Prandtl number has only a marginal effect on the flow and heat transfer.

In this study, MHD natural convection flow and heat transfer in a vertical enclosure with an off-centred partition were investigated numerically using the polynomial differential quadrature (PDQ) method [11–13]. The PDQ method is an efficient discretisation technique used to obtain accurate numerical solutions using a smaller number of grid points than with low-order methods such as finite-difference, finite element and finite volume methods.

2. Mathematical formulation

A schematic of the system with the coordinates and boundary conditions is shown in Fig. 1. The square enclosure with a partition is bounded by two isothermal vertical walls at temperatures T_H and T_C and by two horizontal adiabatic walls.

The dimensionless variables are defined as follows:

$$x = \frac{x^*}{L},\ y = \frac{y^*}{L},\ u = \frac{u^*}{\alpha/L},\ v = \frac{v^*}{\alpha/L},$$

$$p = \frac{L^2}{\rho_o \alpha^2}\left(p^* + \rho_o g y^*\right),\ T = \frac{T^* - T_C}{T_H - T_C} \tag{1}$$

where u^* and v^* are the dimensional velocity components, p^* is the dimensional pressure, T^* is the dimensional temperature, ρ_o is the fluid density at temperature T_C and α is the thermal diffusivity of the fluid.

The flow is considered to be steady, two dimensional and laminar. Neglecting displacement currents, induced magnetic field, dissipation and Joule heating, and using the Boussinesq approximation, the following governing equations can be obtained in the non-dimensional stream function–vorticity form:

$$\frac{\partial^2\psi}{\partial x^2} + \frac{\partial^2\psi}{\partial y^2} = -\omega \tag{2}$$

$$u\frac{\partial\omega}{\partial x} + v\frac{\partial\omega}{\partial y} = \mathrm{Pr}\left(\frac{\partial^2\omega}{\partial x^2} + \frac{\partial^2\omega}{\partial y^2}\right) + \mathrm{Ra}\,\mathrm{Pr}\frac{\partial T}{\partial x} + \mathrm{Ha}^2\mathrm{Pr}\left(\delta\frac{\partial u}{\partial x} - \frac{\partial v}{\partial x} + \delta^2\frac{\partial u}{\partial y} - \delta\frac{\partial v}{\partial y}\right),\ \delta = B_y/B_x \tag{3a}$$

or

$$u\frac{\partial\omega}{\partial x} + v\frac{\partial\omega}{\partial y} = \mathrm{Pr}\left(\frac{\partial^2\omega}{\partial x^2} + \frac{\partial^2\omega}{\partial y^2}\right) + \mathrm{Ra}\,\mathrm{Pr}\frac{\partial T}{\partial x} + \mathrm{Ha}^2\mathrm{Pr}\left(\delta^2\frac{\partial u}{\partial x} - \delta\frac{\partial v}{\partial x} + \delta\frac{\partial u}{\partial y} - \frac{\partial v}{\partial y}\right),\ \delta = B_x/B_y \tag{3b}$$

$$u\frac{\partial T}{\partial x} + v\frac{\partial T}{\partial y} = \frac{\partial^2 T}{\partial x^2} + \frac{\partial^2 T}{\partial y^2} \tag{4}$$

Two equations are given for the vorticity transport equation. Equation (3a) stands for the x-directional magnetic field case ($B_y = 0$), and equation (3b) stands for the y-directional magnetic field case ($B_x = 0$). In these equations, the Prandtl, Rayleigh and Hartmann numbers are defined as:

$$\mathrm{Pr} = \frac{\upsilon}{\alpha},\ \mathrm{Ra} = \frac{g\beta L^3\Delta T^*}{\upsilon\alpha},\ \mathrm{Ha} = LB_x\sqrt{\frac{\sigma}{\mu}}\ (\text{for eq.3a}),\ \mathrm{Ha} = LB_y\sqrt{\frac{\sigma}{\mu}}\ (\text{for eq.3b}) \tag{5}$$

where g is the gravitational acceleration, β is the coefficient of thermal expansion and υ is the kinematic viscosity of the fluid, B is the magnetic induction and σ is electric conductivity.

The boundary conditions for the problem are:

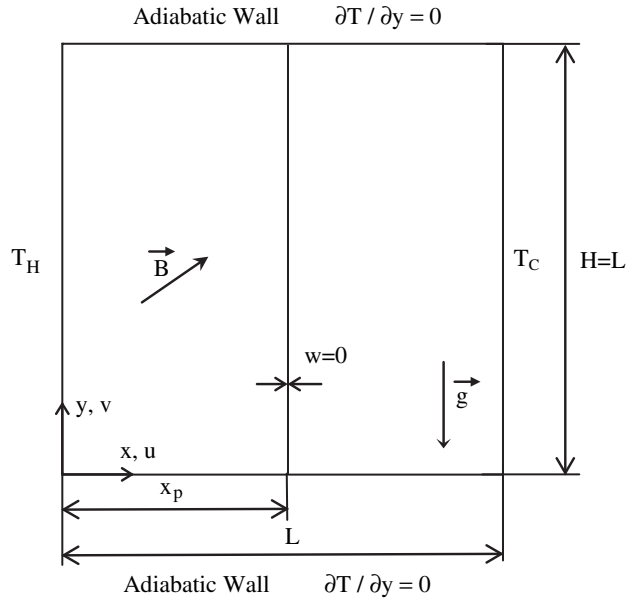

Fig. 1. Geometry and the coordinate system.

$$\psi(x,0)=0,\ \psi(x_p,y)=0,\ \psi(x,1)=0,\ \psi(0,y)=0,\ \psi(1,y)=0 \qquad (6)$$

$$\frac{\partial T}{\partial y}\Big|_{x,0}=0,\ T\left(x_p^-,y\right)=T\left(x_p^+,y\right),\ \frac{\partial T}{\partial x}\Big|_{x_p^-,1}=\frac{\partial T}{\partial x}\Big|_{x_p^+,1},\ \frac{\partial T}{\partial y}\Big|_{x,1}=0,\ \frac{\partial T}{\partial x}\Big|_{0,y}=-1,\ T(0,y)=1,\ T(1,y)=0 \qquad (7)$$

Physically, there is no boundary condition for the vorticity. But an expression can be written from Taylor series expansion of the stream function equation as $\omega_{wall}=-\partial^2\psi/\partial\eta^2$, where η is the outward variable normal to the surface [14].

3. Results and discussions

Because equations (2–4) are coupled and non-linear partial differential equations, they are solved numerically. The governing equations discretised by employing the PDQ method become as follows:

$$\sum_{k=0}^{N_x} b_{i,k}\psi_{k,j}+\sum_{k=0}^{N_y}\overline{b}_{j,k}\psi_{i,k}=-\omega_{i,j} \qquad (8)$$

$$\sum_{k=0}^{N_y}\overline{a}_{j,k}\psi_{i,k}\sum_{k=0}^{N_x}a_{i,k}\omega_{k,j}-\sum_{k=0}^{N_x}a_{i,k}\psi_{k,j}\sum_{k=0}^{N_y}\overline{a}_{j,k}\omega_{i,k}=\mathrm{Ra}\ \mathrm{Pr}\left[\sum_{k=0}^{N_x}a_{i,k}T_{k,j}\right]+\mathrm{Pr}\left[\sum_{k=0}^{N_x}b_{i,k}\omega_{k,j}+\sum_{k=0}^{N_y}\overline{b}_{j,k}\omega_{i,k}\right]+\mathrm{Ha}^2\mathrm{Pr}(1+\delta)\left[\sum_{k=0}^{N_x}b_{i,k}\psi_{k,j}+\delta\sum_{k=0}^{N_y}\overline{b}_{j,k}\psi_{i,k}\right]\quad(\text{Eq. 3a}) \qquad (9a)$$

Table 1
Grid independency test.

Mesh size	Nu_a	$\lvert\psi\rvert_{max}$
18×18	4.25	11.6
22×22	4.28	11.8
26×26	4.32	11.8
30×30	4.32	11.8

$$\sum_{k=0}^{N_y}\overline{a}_{j,k}\psi_{i,k}\sum_{k=0}^{N_x}a_{i,k}\omega_{k,j}-\sum_{k=0}^{N_x}a_{i,k}\psi_{k,j}\sum_{k=0}^{N_y}\overline{a}_{j,k}\omega_{i,k}=\mathrm{Ra}\ \mathrm{Pr}\left[\sum_{k=0}^{N_x}a_{i,k}T_{k,j}\right]+\mathrm{Pr}\left[\sum_{k=0}^{N_x}b_{i,k}\omega_{k,j}+\sum_{k=0}^{N_y}\overline{b}_{j,k}\omega_{i,k}\right]+\mathrm{Ha}^2\mathrm{Pr}(1+\delta)\left[\delta\sum_{k=0}^{N_x}b_{i,k}\psi_{k,j}+\sum_{k=0}^{N_y}\overline{b}_{j,k}\psi_{i,k}\right]\quad(\text{Eq. 3b}) \qquad (9b)$$

$$\sum_{k=0}^{N_y}\overline{a}_{j,k}\psi_{i,k}\sum_{k=0}^{N_x}a_{i,k}T_{k,j}-\sum_{k=0}^{N_x}a_{i,k}\psi_{k,j}\sum_{k=0}^{N_y}\overline{a}_{j,k}T_{i,k}=\left[\sum_{k=0}^{N_x}b_{i,k}T_{k,j}+\sum_{k=0}^{N_y}\overline{b}_{j,k}T_{i,k}\right] \qquad (10)$$

where the indices i and j indicate a grid point, and N_x and N_y represent the total number of grid points in x and y directions, respectively. The following non-uniform grid distribution was adapted to the present study:

$$x_i=\frac{1}{2}\left[1-\cos\left(\frac{i}{N_x}\pi\right)\right],\quad i=0,1,2,\ \ldots,\ N_x\,y_j=\frac{1}{2}\left[1-\cos\left(\frac{j}{N_y}\pi\right)\right],\quad j=0,1,2,\ \ldots,\ N_y \qquad (11)$$

The points in this grid system are more closely spaced in regions near the walls where the higher velocity and temperature gradients are expected to develop. After discretisation by the PDQ method, the governing equations (8–10) were solved by the successive over-relaxation (SOR) iteration method. To ensure convergence of the numerical algorithm, the criterion $|\Phi_{i,j}^m-\Phi_{i,j}^{m+1}|<10^{-5}$ was applied to all dependent variables over the solution domain where Φ represents a dependent variable (ω, ψ, T) and the index m indicates the current iteration.

A series of grid systems of up to 30×30 points were employed to obtain a grid-independent mesh size. The results suggest that when the mesh size is above 26×26, the computed $|\psi|_{max}$, and Nu_a remain the same. The results in the case of $x_p=0.5$, $Ra=10^6$, $Pr=1$ and $Ha=0$ are shown in Table 1. Based on this observation; a non-uniform grid of 30×30 points was used in this study.

To validate the numerical code, the solutions obtained for a non-partitioned square enclosure with the PDQ method for a grid size of 30×30 have also been compared with the benchmark results obtained by de Vahl Davis [15] through a standard finite-difference

Table 2
Validation of the numerical code for a non-partitioned enclosure case.

	$Ra=10^4$		$Ra=10^5$		$Ra=10^6$	
	Vahl Davis	Present	Vahl Davis	Present	Vahl Davis	Present
$\lvert\psi\rvert_{max}$	–	5.07	9.61	9.58	16.75	16.76
Nu_a	2.24	2.24	4.52	4.52	8.80	8.82
Nu_{max}	3.53	3.53	7.72	7.71	17.93	17.53
Nu_{min}	0.59	0.59	0.73	0.73	0.99	0.98

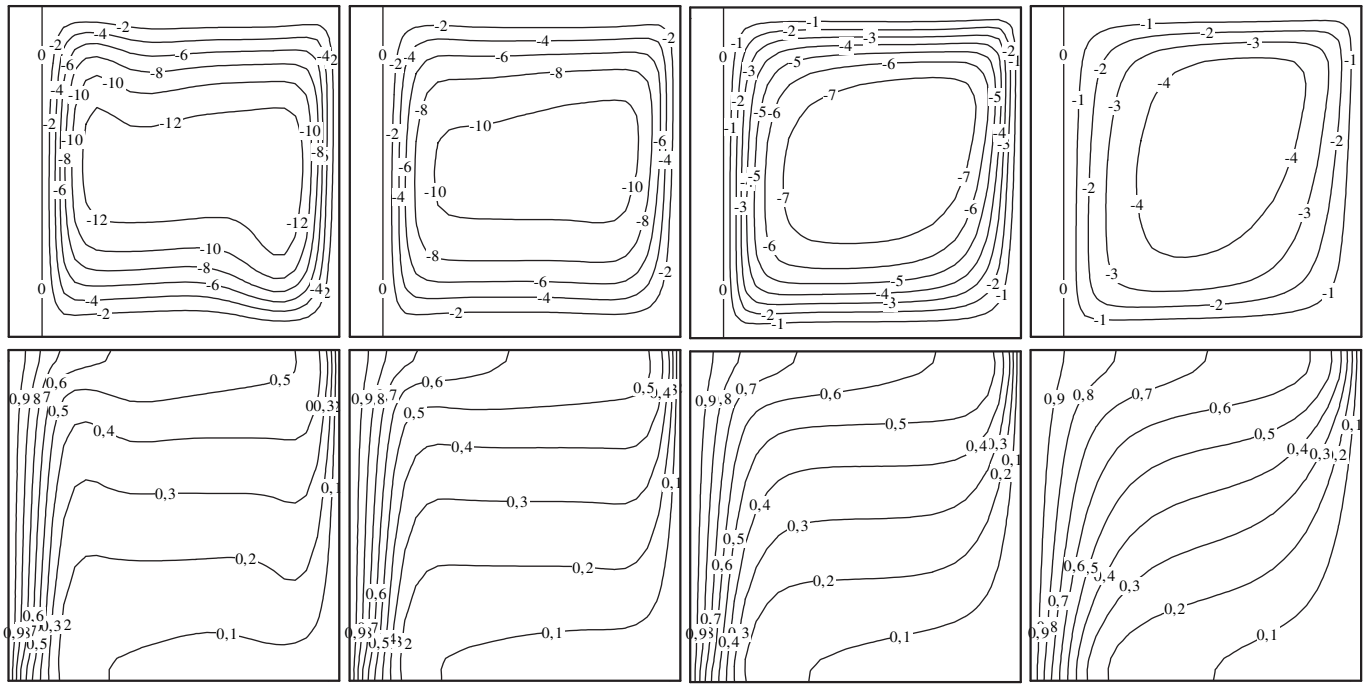

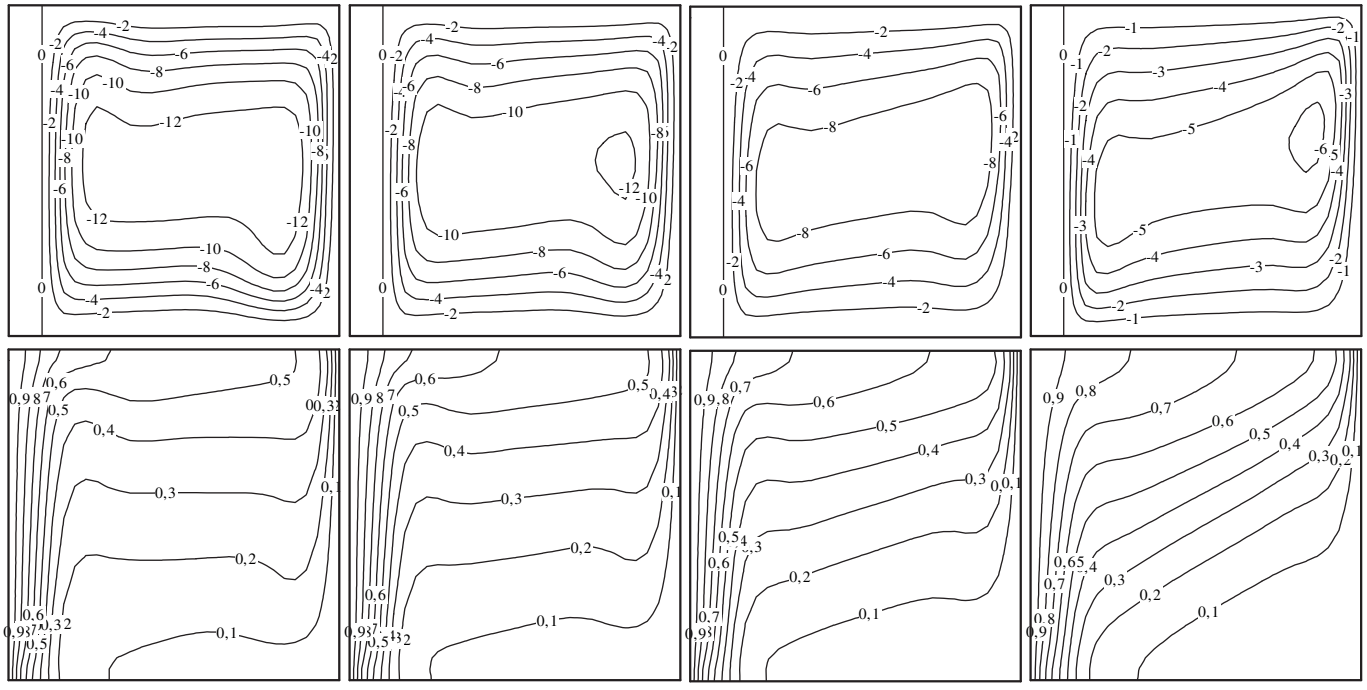

Fig. 2. Streamlines and isotherms for $x_p = 0.1$, $Ra = 10^6$ and $Pr = 1$.

method for grids up to 80×80 (see Table 2). Maximum deviation for the Nu_a and $|\psi|_{max}$ have been found to be within 0.3%.

Computations were carried out for partition locations between 0.1 and 0.5, Rayleigh numbers between 10^4 and 10^6, Prandtl numbers between 0.1 and 10 and Hartmann numbers between 0 and 100. The numerical code did not converge for values of the Rayleigh number higher than 10^6. This is because the flow regime gradually becomes turbulent and hence unsteady for $Ra > 10^6$ [16]. Therefore, 10^6 has been chosen as upper limit for the Rayleigh number to obtain a laminar steady solution.

The buoyancy driven flow and temperature fields inside the enclosure are given by means of streamlines and isotherms in Figs. 2–4

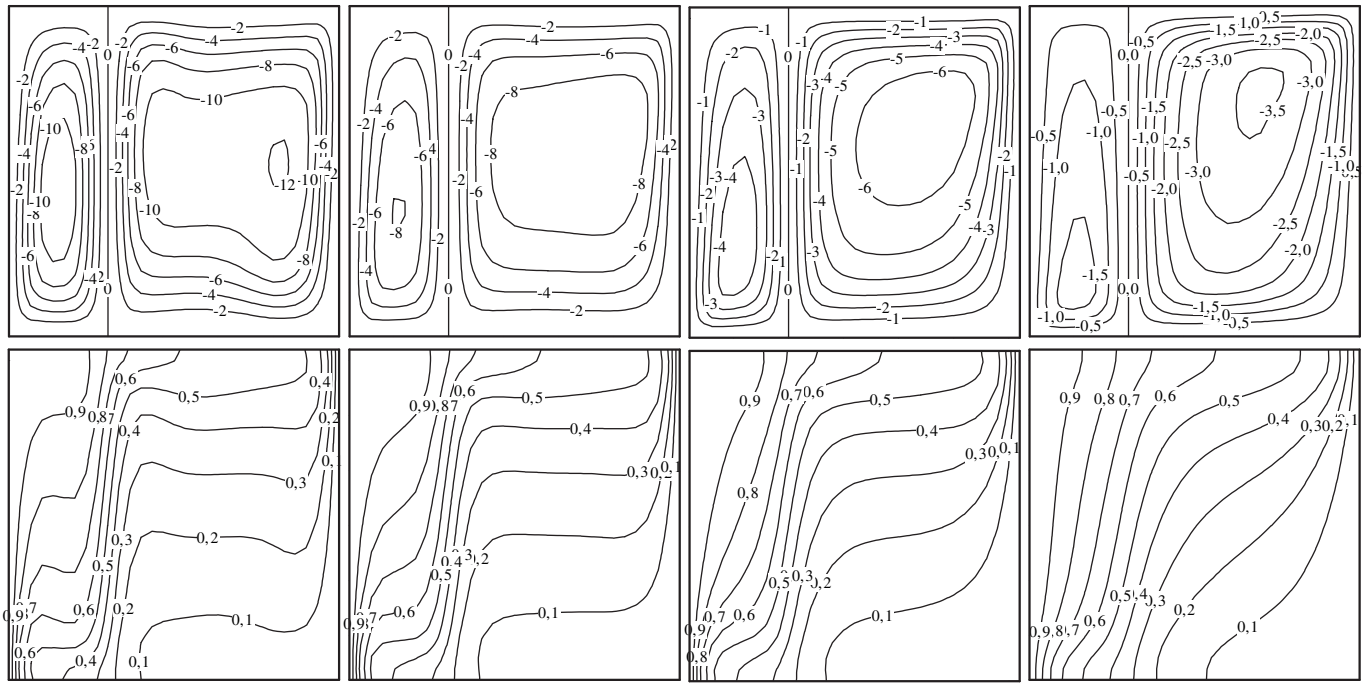

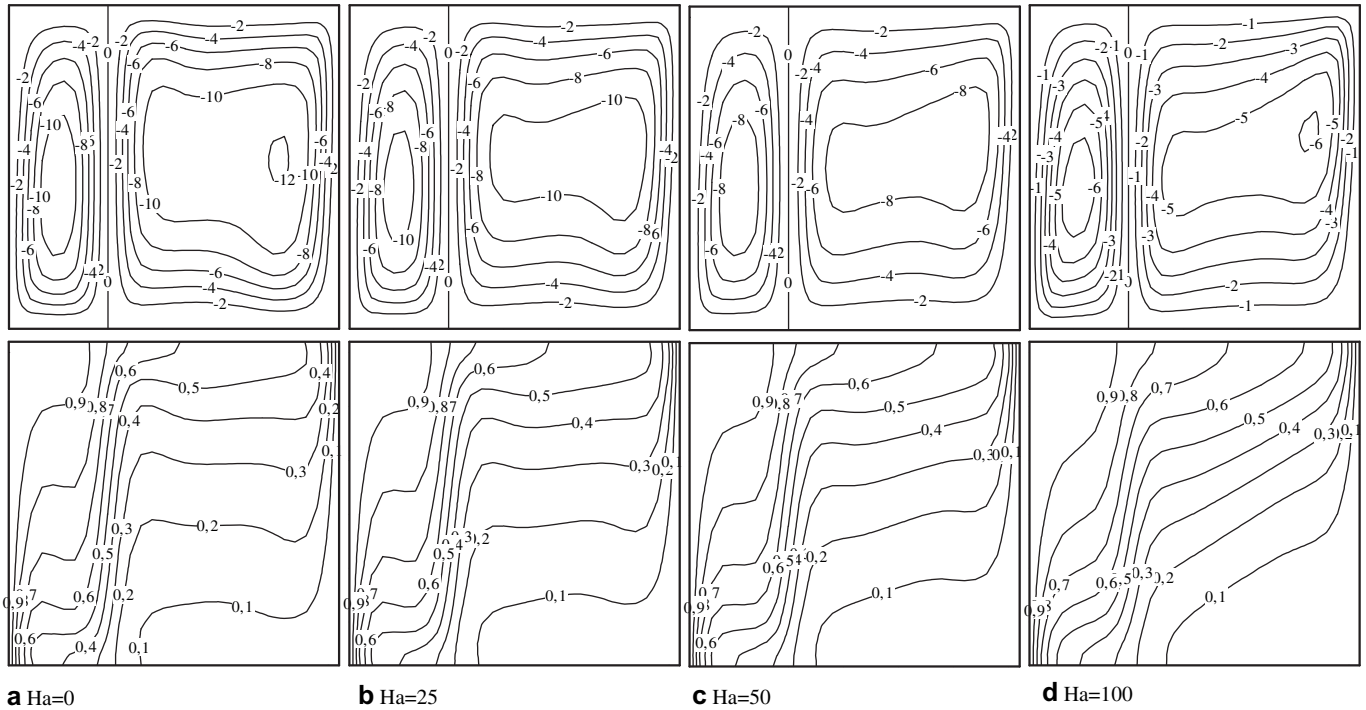

Fig. 3. Streamlines and isotherms for $x_p = 0.3$, $Ra = 10^6$ and $Pr = 1$.

for horizontally and vertically oriented magnetic fields. As may be observed, the flow patterns on both regions of the enclosure are single-cellular. In addition, a boundary layer flow regime exists in the flow fields. This is clear from increasing steepness of the velocity and temperature profiles near the walls, as well as the existence of a plateau in the core regions on either side of the partition. As the Hartmann number is increased, circulation strength decreases considerably. However, with increasing Hartmann number, centres of the circulation cells are shifted toward the regions where the development of the boundary layers starts (in the lower and upper corners of the left and right regions of the enclosure, respectively). This is mainly because the positions of the circulation centres are dependent on the thickness of the boundary layers. For high values of Hartmann numbers, the thicknesses of the boundary layers are larger because of

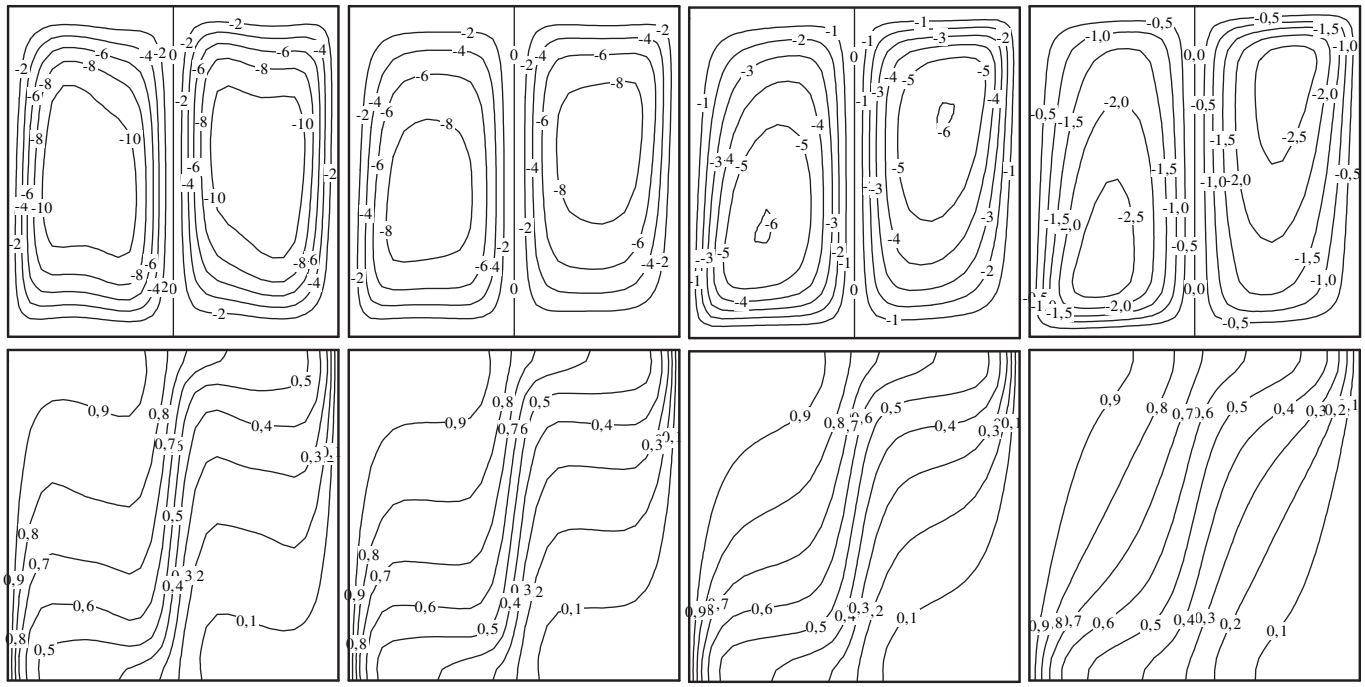

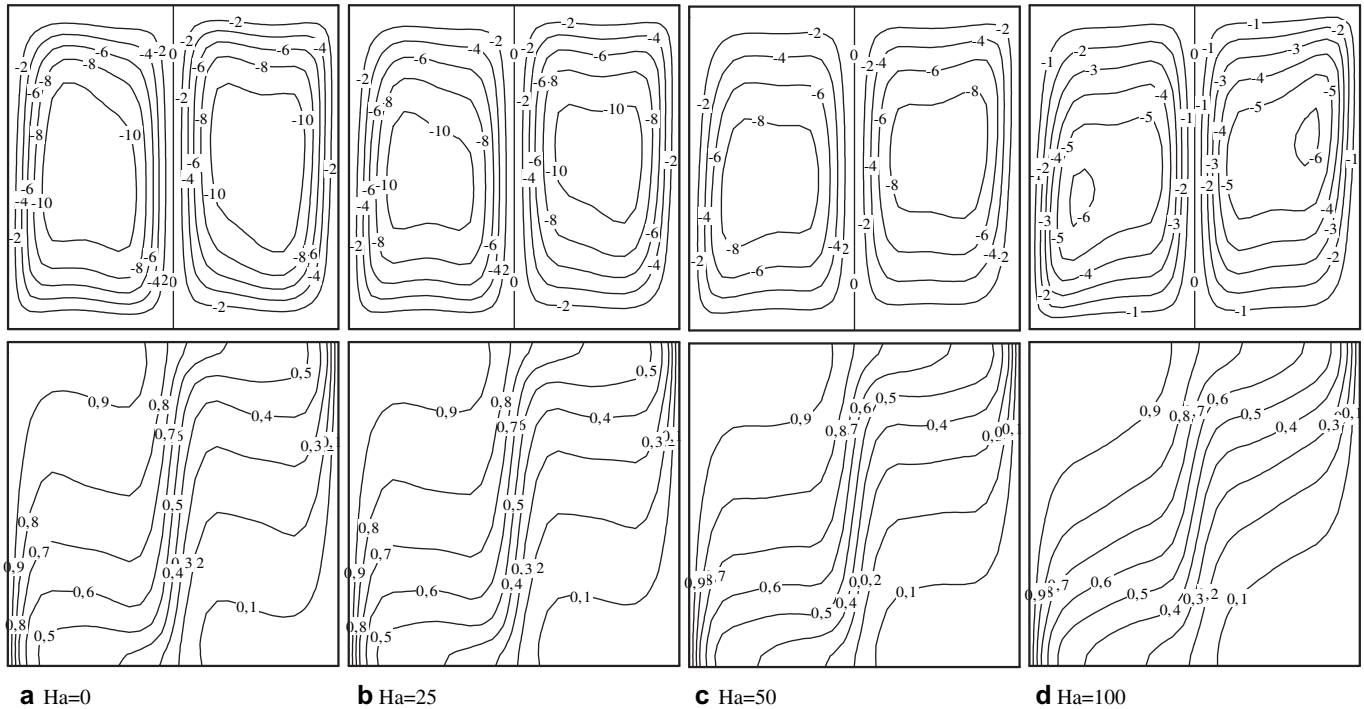

Fig. 4. Streamlines and isotherms for $x_p = 0.5$, $Ra = 10^6$ and $Pr = 1$.

the higher retarding effect of magnetic field on circulation, and, therefore, the circulation centres become closer to the regions where the development of the boundary layers starts. It may also be observed from Figs. 2–4 that with decreasing distance between the partition and the hot wall, convective circulation weakens in the smaller zone. This is clear from nearly parallel isotherms to the vertical walls in the smaller zone. Conversely, convective circulation strengthens in the bigger zone with decreasing distance between hot wall and partition.

The local Nusselt number along the hot surface of the enclosure is presented in Fig. 5. The Nusselt number attains its maximum value close to the leading edge of the hot surface and decreases in the direction of increasing y. This is expected, since the leading edge of the hot surface is washed by fluid cooled by the partition.

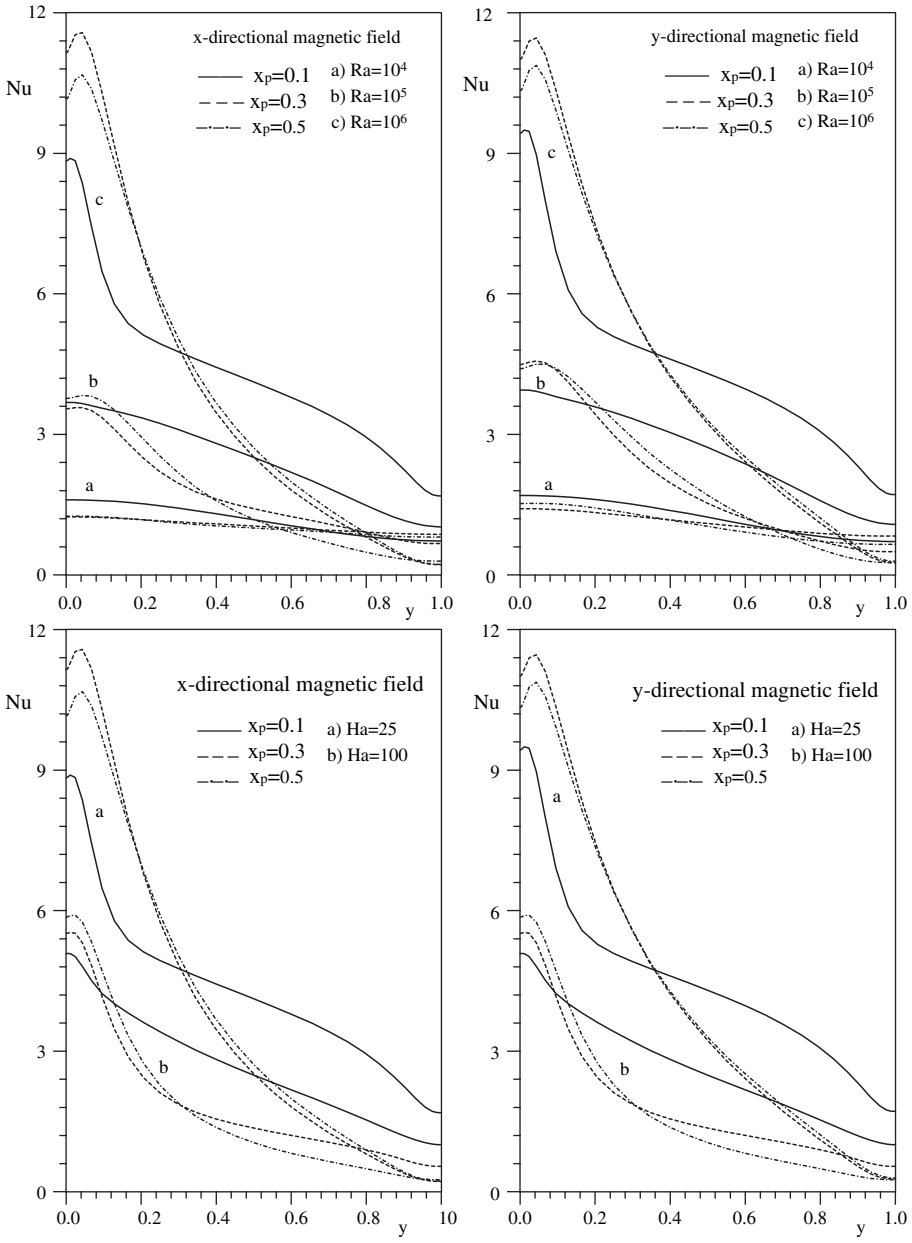

Fig. 5. Variation of the local Nusselt number along the hot wall for $Pr = 1$.

Temperature of the fluid moving up the hot surface increases, and, therefore, the local heat transfer rate decreases along the hot surface. For the low Rayleigh numbers, heat transfer rate is almost constant because of the dominant conduction regime. As convection becomes stronger with increasing Ra, heat transfer rate shows an increasing trend. Because of the retarding effect of magnetic field on flow and therefore on convection, the local Nusselt number decreases significantly under the influence of magnetic field. It may also be observed from the results that the *x*-directional magnetic field yields lower local Nusselt numbers than those for the *y*-directional magnetic field, because the main flow and the retarding effect of *x*-directional magnetic field on flow are in the *y* direction. As the partition diverges from the hot wall, the local Nusselt number represents sharper changes due to gradually strengthening circulation in the left zone and takes lower values for most parts of the hot wall due to gradually weakening circulation in the right zone, which dominates flow and heat transfer in the enclosure.

Variation of the average Nusselt number with the Rayleigh and Prandtl numbers is shown in Fig. 6 for various values of partition location and magnetic field strength. As can be seen, damping is highest for higher strengths of the magnetic field. However, the maximum decrease is for $Ra = 10^5$, especially for low values of the Hartmann number. This is mainly because of the convection strength. For low Rayleigh numbers, convection is weak; hence the retarding effect of the magnetic field has little impact. On the other hand, for high values of the Rayleigh number convection intensity is rather high and magnetic field strength remains relatively weak in retarding the flow. Because buoyancy force is in the same order with Lorentz force for modest levels of the Rayleigh number, the magnetic field suppresses flow more with increasing magnetic field strength and causes higher decreases in the average Nusselt number. As the partition moves away from the hot wall, convection intensity weakens on the right region, which is more effective on flow and

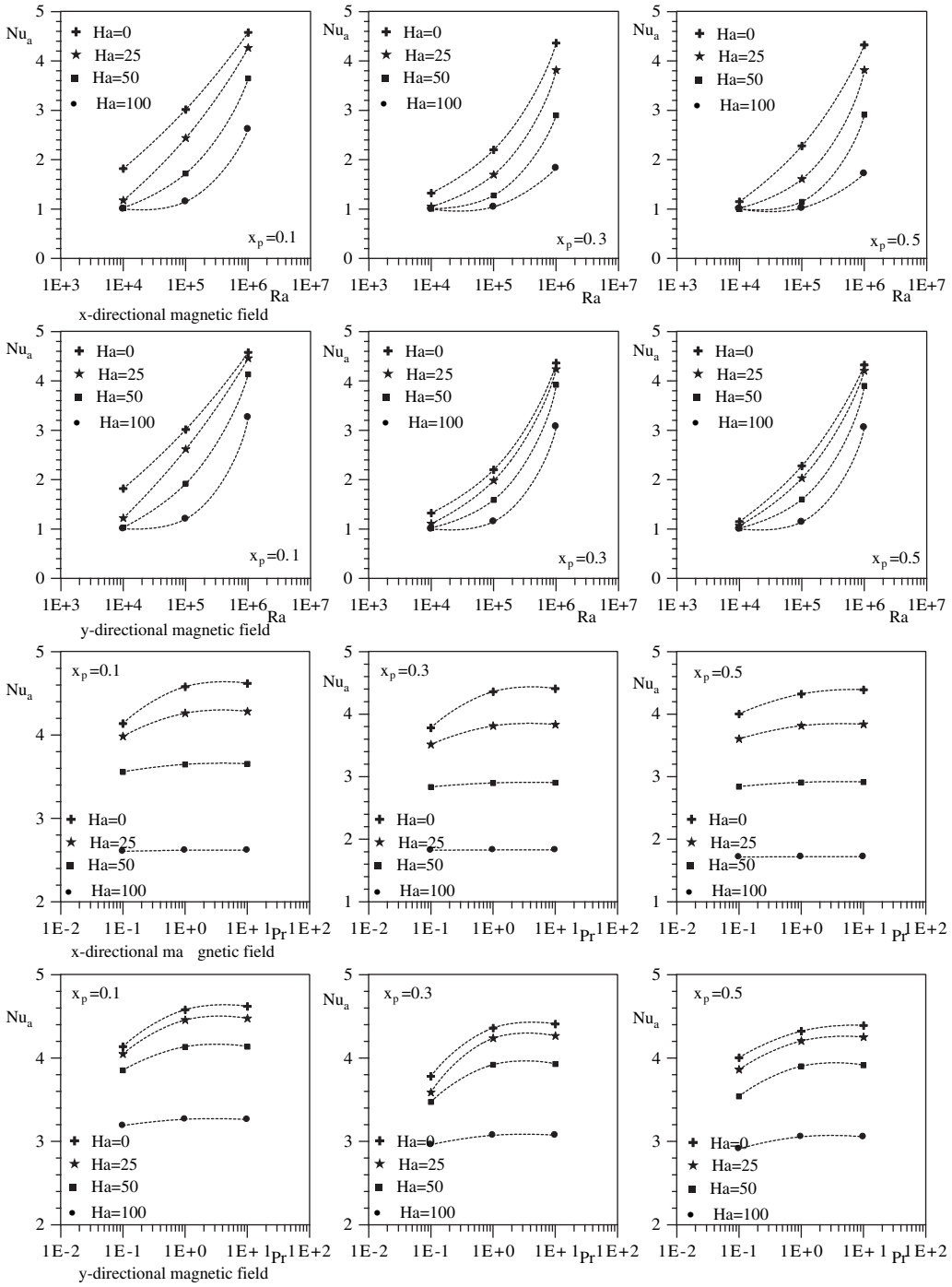

Fig. 6. Variation of the average Nusselt number with the Rayleigh and Prandtl numbers.

heat transfer. Therefore, average heat transfer rate takes lower values and magnetic field intensity becomes more effective on flow and heat transfer. Consequently, the average Nusselt number decreases more with increasing Ha number, especially for high values of the Ra number. The effect of the partition location on natural convection weakens as the partition approaches the centre of the enclosure. The *x*-directional magnetic field retards the flow in the *y* direction, which is the main flow direction; therefore, the *x*-directional magnetic field is more effective in weakening convection. The numerical calculations show that the average heat transfer rate decreases up to 80% in the range of parameters taken into consideration in this study if a centred partition is used in the enclosure and an *x*-directional magnetic field is applied. Hence, it can be concluded that the most effective way to reduce heat transfer in an enclosure is to use a centrally located partition that is under an *x*-directional magnetic field. It may also be observed from Fig. 6 that the average Nusselt number increases little with increasing Prandtl number. The main cause of the increase in the average Nusselt number with the Prandtl number is that the thermal boundary layer is embedded in the momentum boundary layer and becomes relatively thinner with increasing Prandtl number.

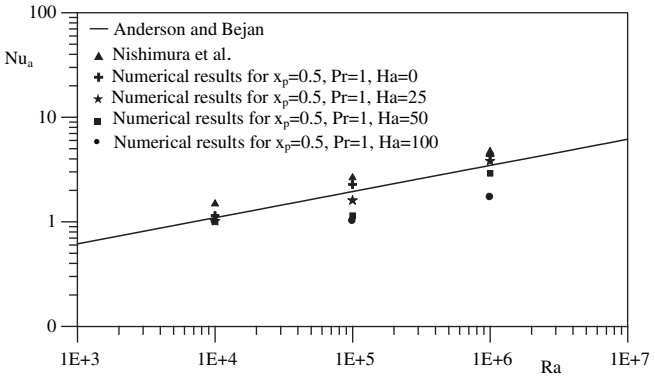

Fig. 7. A comparison for the average Nusselt number.

Various correlations for the average Nusselt number are available in the literature for the partitioned enclosures in the absence of a magnetic field. A correlation for the average Nusselt number based on the experimental results of Anderson and Bejan [1] is given as $\mathrm{Nu_a} = 0.201\mathrm{Ra}^{0.276}(N+1)^{-1/4}$. Here N is the partition number. Another correlation is given by Nishimura et al. [17] as $\mathrm{Nu_a} = 0.297\mathrm{Ra}^{1/4}(N+1)^{-1}$. The comparison of the results with the aforementioned studies for the average Nusselt number is presented in Fig. 7 along with the values of the average Nusselt number for the x-directional magnetic field. It may be observed from Fig. 6 that the numerical results for the average Nusselt number are in good agreement with those of the correlations.

4. Conclusion

The buoyancy-driven magnetohydrodynamic flow in a laterally heated enclosure with a thermally active off-centred partition has been investigated numerically by the PDQ method. The effects of magnetic field as well as the partition location and Rayleigh and Prandtl numbers on flow and heat transfer have been examined. Two different orientations of the magnetic field, x-directional and y directional, were taken into account in the calculations. The results show that the magnetic field suppresses flow, and hence heat transfer, significantly, especially for high values of the Rayleigh number. The results also show that the x-directional magnetic field is more effective in damping convection than the y-directional magnetic field, and the average heat transfer rate decreases with an increase in the distance of the partition from the hot wall. The average heat transfer rate decreases up to 80% if a centred partition is used and an x-directional magnetic field is applied. The computations also show that the Prandtl number has little effect on flow and heat transfer.

References

[1] R. Anderson, A. Bejan, Heat transfer through single and double vertical walls in natural convection: theory and experiment, International Journal of Heat and Mass Transfer 24 (1983) 1611–1620.
[2] C.J. Ho, Y.L. Yih, Conjugate natural heat transfer in a air-filled rectangular cavity, International Communication in Heat and Mass Transfer 14 (1987) 91–100.
[3] T.W. Tong, F.M. Gerner, Natural convection in partitioned air-filled rectangular enclosures, International Communication in Heat and Mass Transfer 10 (1986) 99–108.
[4] D.M.C. Dzodzo, M.B. Dzodzo, M.D. Pavlovic, Laminar natural convection in a fully partitioned enclosure containing fluid with nonlinear thermophysical properties, International Journal of Heat and Fluid Flow 20 (1999) 614–623.
[5] S.M. Elsherbiny, K.G.T. Holland, G.T. Raithby, Effect of the thermal boundary condition on natural convection in vertical and inclined air layers, in: , Proc. 20th ASME-AIChE Natn. Heat Transfer Conference, vol. 16, 1981, pp. 127–133 Milwaukee, Wisconsin HT.
[6] S. Acharya, C.H. Tsang, Natural convection in a fully partitioned inclined enclosure, Numerical Heat Transfer 8 (1985) 407–428.
[7] K. Kahveci, Natural convection in a partitioned vertical enclosure heated with a uniform heat flux, ASME Journal of Heat Transfer 129(6) (2007) 717–726.
[8] K. Kahveci, Numerical simulations of natural convection in a partitioned enclosure, International Journal of Numerical Methods for Heat and Fluid Flow 17 (4) (2007) 439–456.
[9] K. Kahveci, A differential quadrature solution of natural convection in an enclosure with a finite thickness partition, Numerical Heat Transfer, Part A 51 (10) (2007) 979–1002.
[10] K. Kahveci, S. Öztuna, A differential quadrature solution of MHD natural convection in an inclined enclosure with a partition, ASME Journal of Fluids Engineering 130 (2008) 021102.
[11] C. Shu, Differential Quadrature and its Application in Engineering, Springer-Verlag, 2000.
[12] R.E. Belman, B.G. Kashef, J. Casti, Differential quadrature: a technique fort he rapid solution of nonlinear partial differential equations, Journal of Computational Physics 10 (1972) 40–52.
[13] C. Shu, Generalised differential-integral quadrature and application to the simulation of incompressible viscous flows including parallel computation, Ph.D thesis, University of Glasgow, 1992.
[14] D. Elkaim, M. Reggio, R. Camarero, Simulating two-dimensional turbulent flow by using k–ε model and the vorticity–stream function formulation, International Journal of Numerical Methods in Fluids 14 (1992) 961–980.
[15] G. de Vahl Davis, Natural convection in a square cavity, International Journal of Numerical Methods Fluids 3 (1983) 249–264.
[16] N.C. Markatos, K.A. Pericleous, Laminar and turbulent natural convection in an enclosed cavity, International Journal of Heat and Mass Transfer 27 (5) (1984) 755–772.
[17] T. Nishimura, M. Shiraishi, F. Nagasawa, Y. Kawamura, Natural convection heat transfer in enclosures with multiple vertical partitions, International Journal of Heat and Mass Transfer 31 (1998) 1679–1698.